# Superconducting state in a crystal of low symmetry: Impurity effect in an extended *s*-wave superconductor with nodes in the excitation gap

K. Yamashita and D. S. Hirashima
*Department of Physics, Nagoya University, Nagoya 464-8602, Japan*
(Received 1 December 2008; published 15 April 2009)

It is argued that an extended *s*-wave superconducting state having order parameter that changes its sign on the Fermi surface is likely to occur in crystals of low symmetry such as organic conductors, if the pairing interaction is of electronic origin. Impurity effects in those superconducting states are then studied. Special attention is paid to the nuclear magnetic relaxation rate $1/T_1$. It is found that impurities give rise to peculiar behavior of $1/T_1$ such as a coherence peak just below the transition temperature *and* $T$-linear variation, caused by impurity-induced finite density of states at the chemical potential, at low temperatures, at moderate impurity concentration.

DOI: 10.1103/PhysRevB.79.144513 PACS number(s): 74.20.Rp, 74.70.Kn, 74.25.Nf

## I. INTRODUCTION

Study of the impurity effect is an important part of the study of superconductivity. One can distinguish an unconventional pairing state from an isotropic *s*-wave one by studying the impurity effect in the superconducting state, for example, because the effect of impurity scattering depends on the symmetry of order parameter. While an isotropic *s*-wave state is robust against nonmagnetic impurity scattering,[1,2] an unconventional pairing state is sensitive to impurity scattering.

Precisely speaking, symmetry of the superconducting order parameter is classified by the irreducible representation of the space group of the crystal where the superconductivity occurs.[3–5] When the total momentum of Cooper pairs vanishes, the irreducible representation of a point group is sufficient to classify symmetry. Usually, order parameter represented by an irreducible representation other than the identity representation is called unconventional. It is often the case that an unconventional superconducting state has a node (nodes) in the excitation gap, which leads to various anomalous behaviors.

A pairing state belonging to the identity representation is called an extended *s*-wave state in this study. Extended *s*-wave states include the isotropic *s*-wave state. An extended *s*-wave state is nodeless in many cases. However, no symmetry requirement prohibits the occurrence of nodes in the excitation gap. Therefore, it is possible that an extended *s*-wave state has order parameter that changes sign on the Fermi surface. Indeed, the impurity effect in an extended *s*-wave state with nodes in the gap was studied by many authors,[6–13] in pursuit of determination of the order parameter symmetry in high-$T_c$ superconductors, and some peculiar behaviors such as the impurity-induced opening of the gap (in the case of sign-changing order parameter) were found.[9–14] However, the order parameter in the high-$T_c$ superconductors turned out to be of *d*-wave symmetry.[15] Moreover, it appears difficult for extended *s*-wave order parameter with sign change to be realized in actual materials. Presumably, that is why the peculiar impurity effect in an extended *s*-wave state (with sign change of the order parameter) has not been further studied.

However, as will be discussed later, extended *s*-wave order parameter with sign-change is likely to occur in crystals of low symmetry if the mechanism of superconductivity is of electronic origin. The purpose of this paper is to discuss this possibility and then to elucidate the impurity effects in those superconducting states, i.e., extended *s*-wave superconducting states with order parameter changing its sign on the Fermi surface.

One of the families of unconventional superconductors is low-dimensional organic conductors.[16] Now, the number of organic superconductors exceeds 100. One of the features of the low-dimensional organic conductors is its low symmetry of crystals.[17] A typical space group describing crystals of organic conductors is $P\bar{1}$. The crystal system is triclinic, and has no symmetry other than the inversion symmetry. The corresponding point group $C_i$ has only two irreducible representations. One is the identity representation corresponding to an even-parity (extended *s*-wave) pairing state, and the other representation corresponds to an odd-parity state. In these systems, only the distinction between even- and odd-parity pairing is relevant, and the further classification is irrelevant at least from a group-theoretical point of view.

Mechanism of superconductivity in low-dimensional organic conductors has been studied extensively.[16,18,19] In some of the materials, the superconducting phase is in close proximity of the antiferromagnetic long-range ordered phase, which implies that the superconductivity is induced by antiferromagnetic spin fluctuations.[20–22] It has also been argued that enhanced charge fluctuations may cause superconductivity in some of organic conductors.[23–27] At any rate, if the mechanism of superconductivity is of electronic origin, the resultant superconducting order parameter is likely to have substantial wave-vector dependence. Then, it is highly possible that the order parameter is of the extended *s*-wave symmetry *and* has nodes in the excitation gap.

In Sec. II, we explicitly introduce a model that gives an extended *s*-wave superconducting state, and then study the impurity effect in the superconducting state in Sec. III. In addition to the transition temperature and the density of states, we discuss the nuclear magnetic relaxation time. Section IV is devoted to summary and discussion.

 

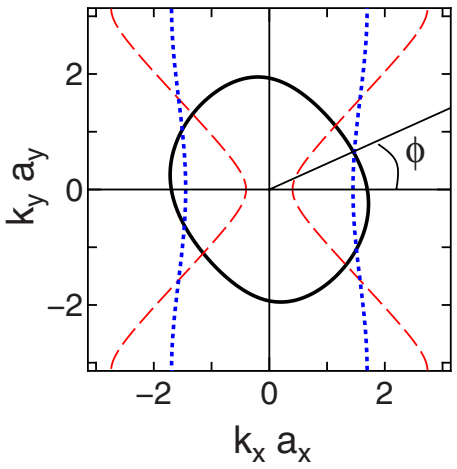


FIG. 1. (Color online) Fermi surface (solid curve) in the quarter-filled case, $n=0.5$: $t_x:t_y:t'=1.0:0.8:0.2$. Zeros in the superconducting gap are also shown: dashed curves are for $v_y=v_x$, and dotted curves are for $v_y=0.4v_x$.

## II. MODEL

We consider an electron system on an anisotropic triangular lattice. The Hamiltonian is given by

$$\mathcal{H}=\sum_{\boldsymbol{k},\sigma}[\epsilon(\boldsymbol{k})-\mu]c^{\dagger}_{\boldsymbol{k}\sigma}c_{\boldsymbol{k}\sigma}=\sum_{\boldsymbol{k},\sigma}\xi(\boldsymbol{k})c^{\dagger}_{\boldsymbol{k}\sigma}c_{\boldsymbol{k}\sigma}, \tag{1}$$

where

$$\epsilon(\boldsymbol{k})=-2\sum_{\mu=x,y}t_\mu\cos k_\mu a_\mu-2t'\cos(k_x a_x+k_y a_y), \tag{2}$$

$a_\mu$ is the lattice constant in the $\mu$ direction, $c_{\boldsymbol{k}\sigma}$ ($c^{\dagger}_{\boldsymbol{k}\sigma}$) is the annihilation (creation) operator of an electron with wave-vector $\boldsymbol{k}$ and spin $\sigma$. When $t_x=t_y=t'$, the problem becomes equivalent to that defined on a triangular lattice, but here we study the case with $t_y=0.8t_x$ and $t'=0.2t_x$ unless otherwise stated. The system is then has no symmetry other than the inversion symmetry. The Fermi surface in the quarter-filled case, $n=0.5$, which is considered in this paper, is shown in Fig. 1. An anisotropic triangular lattice is often considered in the study of organic conductors. Here, we study it as a typical system that has no symmetry other than the inversion one, and do not consider a specific material.

We assume here that the effective attractive interaction leading to superconductivity is of electronic origin. One of the features of such effective interaction is its substantial wave-vector dependence. This means that, in real space, the effective interaction works mainly between electrons at different sites. In this paper, we do not further specify the mechanism of the attractive interaction, but phenomenologically introduce attractive interaction working between electrons at the nearest neighbor sites. Projecting out that part relevant for the formation of Cooper pairs, the effective interaction is given by

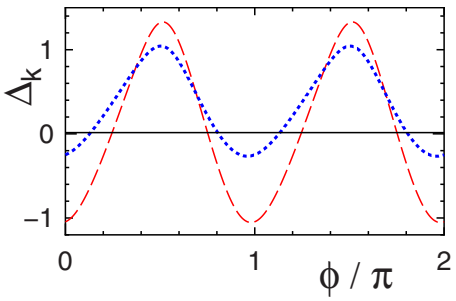


FIG. 2. (Color online) Angular dependence of the gap parameter $\Delta_{\boldsymbol{k}}$ (at $T\to T_c^{(0)}$) on the Fermi surface. For the definition of $\phi$, see Fig. 1. Dashed curve is the result for $v_y=v_x$, and dotted curve for $v_y=0.4v_x$. Gap parameter is normalized so that $\Delta_x=1$.

$$\mathcal{V}=\frac{1}{N}\sum_{\boldsymbol{k},\boldsymbol{k}'}\left[\sum_{\mu=x,y}v_\mu\cos(k_\mu)\cos(k'_\mu)\right]c^{\dagger}_{-\boldsymbol{k}'\downarrow}c^{\dagger}_{\boldsymbol{k}'\uparrow}c_{\boldsymbol{k}\uparrow}c_{-\boldsymbol{k}\downarrow}, \tag{3}$$

where $N$ is the total number of lattice points, and the interaction strength $v_\mu$ may depend on the direction. Here and in the following, we put $a_\mu=1$ for simplicity.

In the mean-field approximation, the gap $\Delta_{\boldsymbol{k}}$ is expressed as

$$\Delta_{\boldsymbol{k}}=\Delta_x(T)\cos k_x+\Delta_y(T)\cos k_y, \tag{4}$$

and the gap equation is given by

$$\begin{vmatrix} 1-\frac{v_x}{N}\sum_{\boldsymbol{k}}\cos^2 k_x\Theta(\boldsymbol{k}) & -\frac{v_x}{N}\sum_{\boldsymbol{k}}\cos k_x\cos k_y\Theta(\boldsymbol{k}) \\ -\frac{v_y}{N}\sum_{\boldsymbol{k}}\cos k_x\cos k_y\Theta(\boldsymbol{k}) & 1-\frac{v_y}{N}\sum_{\boldsymbol{k}}\cos^2 k_y\Theta(\boldsymbol{k}) \end{vmatrix}=0, \tag{5}$$

where $\Theta(\boldsymbol{k})=[2E(\boldsymbol{k})]^{-1}\tanh\beta E(\boldsymbol{k})/2$ and $E(\boldsymbol{k})=\sqrt{\xi(\boldsymbol{k})^2+\Delta_{\boldsymbol{k}}^2}$. In this study, we put $T_c^{(0)}=0.05t_x$, where $T_c^{(0)}$ is the transition temperature in the clean limit. We determine the values of $v_x$ and $v_y$ so that $T_c^{(0)}=0.05t_x$ is achieved.

In Fig. 1, we also show the zero in the gap $\Delta_{\boldsymbol{k}}$ at $T\to T_c^{(0)}$. At $v_y=v_x$, $r_y(T_c^{(0)})=\Delta_y(T)/\Delta_x(T)|_{T\to T_c^{(0)}}=-0.92$, and the gap is close to the $d$-wave one and has nodes near the diagonals of the Brillouin zone. If $r_y$ were equal to $-1$, the gap would be of pure $d$-wave symmetry, but the $s$-wave component is mixed, because there is no clear distinction between $s$- and $d$-wave symmetries in the present case. At $v_y=0.4v_x$, $r_y$ decreases [$r_y(T_c^{(0)})=-0.12$], i.e., the $s$-wave component mixes more, and nodes in $\Delta_{\boldsymbol{k}}$ are near the line $k_x=\pi/2$. However, nodes in the excitation gap still remain. Angular dependence of the gap function $\Delta_{\boldsymbol{k}}$ on the Fermi surface is shown in Fig. 2; here we put $\Delta_x(T\to T_c^{(0)})=1$. It can be seen that order parameter changes its sign in both cases. An important parameter characterizing the anisotropy of the gap is defined by

$$A_0=1-\left.\frac{\langle\langle\Delta_{\boldsymbol{k}}\rangle\rangle^2}{\langle\langle\Delta_{\boldsymbol{k}}^2\rangle\rangle}\right|_{T\to T_c^{(0)}}, \tag{6}$$

where $\langle\langle\cdots\rangle\rangle$ stands for the average on the Fermi surface. For an isotropic gap, $A_0=0$, and for a purely $d$-wave gap, e.g.,

$A_0=1$. For $v_y=v_x$, $A_0=0.96$, and for $v_y=0.4v_x$, $A_0=0.58$.

## III. IMPURITY EFFECT

Nonmagnetic impurities are introduced as local potential scatterers as usual. In organic conductors, the impurity potential must be rather weak. It is therefore sufficient to consider the Born limit, but we also briefly discuss the $T$-matrix approximation in Appendix A for completeness. Using the Nambu representation, the $(2\times 2)$ Green's function in the clean limit is expressed as

$$G^{(0)}(\boldsymbol{k},i\epsilon_n)=(i\epsilon_n-\xi(\boldsymbol{k})\sigma_z-\Delta_{\boldsymbol{k}}\sigma_x)^{-1}, \tag{7}$$

where $\epsilon_n$ is Matsubara frequency for a Fermion and $\sigma_\mu$ is a Pauli matrix. Effect of impurity scattering is expressed as the self-energy correction $\Sigma(i\epsilon_n)$,

$$G(\boldsymbol{k},i\epsilon_n)=[G^{(0)}(\boldsymbol{k},i\epsilon_n)^{-1}-\Sigma(i\epsilon_n)]^{-1}=[i\tilde{\epsilon}(i\epsilon_n)-\xi(\boldsymbol{k},i\epsilon_n)\sigma_z-\tilde{\Delta}_{\boldsymbol{k}}(i\epsilon_n)]^{-1}. \tag{8}$$

In the Born approximation, we obtain

$$i\tilde{\epsilon}(i\epsilon_n)=i\epsilon_n+n_iu^2g_0(i\epsilon_n), \tag{9}$$

and

$$\tilde{\Delta}_{\boldsymbol{k}}(i\epsilon_n)=\Delta_{\boldsymbol{k}}+n_iu^2g_x(i\epsilon_n), \tag{10}$$

where

$$g_0(z)=\frac{1}{N}\sum_{\boldsymbol{k}}\frac{i\tilde{\epsilon}(z)}{D(\boldsymbol{k},z)}, \tag{11}$$

$$g_x(z)=\frac{1}{N}\sum_{\boldsymbol{k}}\frac{\tilde{\Delta}_{\boldsymbol{k}}(z)}{D(\boldsymbol{k},z)}, \tag{12}$$

$D(\boldsymbol{k},i\epsilon_n)=\tilde{\epsilon}(i\epsilon_n)^2+\xi(\boldsymbol{k})^2+\tilde{\Delta}_{\boldsymbol{k}}(i\epsilon_n)^2$, $n_i$ is the concentration of impurities, and $u$ is the strength of the impurity potential. Strictly, there also occurs the renormalization of the kinetic energy $\xi_{\boldsymbol{k}}$ (in the absence of the particle-hole symmetry), but we neglect it here, because it is a small effect after all. In addition to Eqs. (9) and (10), we have the gap equation,

$$\Delta_{\boldsymbol{k}}=\frac{1}{N}\sum_{\boldsymbol{k}'}T\sum_n\left(\sum_{\mu=x,y}v_\mu\cos k_\mu\cos k'_\mu\right)\frac{\tilde{\Delta}_{\boldsymbol{k}'}(i\epsilon_n)}{D(\boldsymbol{k}',i\epsilon_n)}. \tag{13}$$

Equations (9), (10), and (13) constitute the self-consistent Born approximation.

### A. Transition temperature

First, we study the impurity effect on the transition temperature. In the normal phase, $\tilde{\epsilon}(i\epsilon_n)\simeq\epsilon_n+\Gamma_B\,\mathrm{sgn}(\epsilon_n)$. Using this, and after a straightforward calculation (see Appendix B), we obtain

$$\Delta T_c=T_c-T_c^{(0)}=-\frac{\pi}{4}A_0\Gamma_B, \tag{14}$$

where $\Gamma_B=\pi N_0n_iu^2$ with $N_0$ being the density of states (per spin) at the Fermi surface in the normal phase, in agreement with the previous results.[28–30] On the other hand, in the dirty limit, $\Gamma_B\gg T_c$ (but $\Gamma_B\ll W$ with $W$ being the band width),

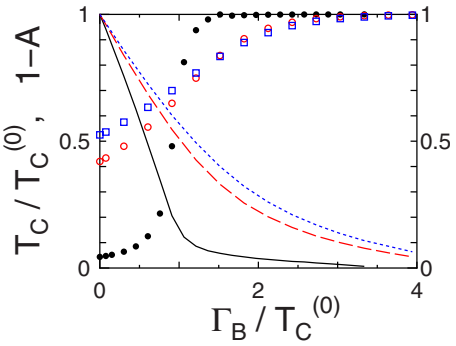


FIG. 3. (Color online) Dependence of the transition temperature $T_c$ on the scattering rate $\Gamma_B$ for different values of $v_y/v_x$: $v_y/v_x$ =1.0 (solid curve), 0.4 (dashed curve), and 0.0 (dotted curve). Also shown is the effective gap isotropy $1-A$ at $T=T_c$ for $v_y/v_x=1.0$ (solid dots), 0.4 (open dots), and 0.0 (open squares).

$$T_c\propto\Gamma_B^{-A_0/(1-A_0)}, \tag{15}$$

$(0\le A_0<1)$.[12,28,30] In Fig. 3, we show the numerical results for dependence of $T_c$ on the impurity concentration. Also shown is the effective gap anisotropy $A$ defined by

$$A=1-\left.\frac{\langle\langle\tilde{\Delta}_{\boldsymbol{k}}(i\pi T)\rangle\rangle^2}{\langle\langle\tilde{\Delta}_{\boldsymbol{k}}(i\pi T)^2\rangle\rangle}\right|_{T\to T_c}, \tag{16}$$

which is experimentally relevant quantity. It can be seen that as the gap becomes effectively isotropic, the dependence of $T_c$ on impurity concentration crossovers from Eq. (14) to Eq. (15).

### B. Density of states

It is well known that impurities give rise to significant change in the quasiparticle density of states in unconventional superconducting states. In an extended $s$-wave superconductor with nodes but with no sign change in the order parameter, a finite gap is readily open in the density of states once an infinitesimal amount of impurities is introduced.[7–9] On the other hand, in a $d$-wave superconductor, which has sign-changing order parameter, impurities cause a finite density of states at the chemical potential (gaplessness).[31–34]

In an extended $s$-wave superconductor with sign-changing order parameter, the density of states changes in a peculiar way as a function of impurity concentration.[9–14] For a fixed temperature (below $T_c$), an infinite amount of impurities results in a finite density of states at $\omega=0$ (at the chemical potential), as in a $d$-wave superconductor. On increasing the impurity concentration, the density of states at $\omega=0$ first increases, but then decreases, and a finite gap opens at $\omega=0$ above critical concentration. The critical concentration $\Gamma_{B,c}$ is determined by[9]

$$\left\langle\left\langle \frac{\Gamma_{B,c}}{|\Delta_{\boldsymbol{k}}+\Gamma_{B,c}|}\right\rangle\right\rangle = 1, \tag{17}$$

in the Born approximation. We have assumed that $\langle\langle\Delta_{\boldsymbol{k}}\rangle\rangle \geq 0$. If the left-hand side (lhs) of Eq. (17) exceeds unity, a finite density of states at $\omega=0$ develops, but if it does not, $N(0)=0$. When $\Delta_{\boldsymbol{k}}+\Gamma_B$ vanishes on a two-dimensional (2D) Fermi surface, the lhs of Eq. (17) logarithmically diverges, and a finite $N(0)$ inevitably results. When $-\Delta_{\min} \leq \Delta_{\boldsymbol{k}} \leq \Delta_{\max}$ on the Fermi surface ($\Delta_{\min}, \Delta_{\max} \geq 0$), the critical concentration is determined roughly by $\Gamma_{B,c} \simeq \Delta_{\min}$. When $\Gamma_B \gtrsim \Delta_{\min}$, a finite gap opens. These facts were already discussed in previous works.[9–14] It should be noted here that $\Delta_{\boldsymbol{k}}$ is not a quantity directly measured in experiments, but $\tilde{\Delta}_{\boldsymbol{k}}(\omega+\mathrm{i}\delta)$ is.

One of the interesting results of the above discussion is that, *in an extended s-wave superconductor, a finite gap in the density of states necessarily develops near $T_c$ unless impurities are completely absent.* This is a straightforward result, but it appears that little attention has been paid to it.

In calculations in the superconducting state, we make further approximations. First, we approximate integrals as

$$\frac{1}{N}\sum_{\boldsymbol{k}} \frac{F(\cos k_x, \cos k_y)}{\tilde{\epsilon}(z)^2+\xi_{\boldsymbol{k}}^2+\tilde{\Delta}_{\boldsymbol{k}}(z)^2} \simeq N_0 \left\langle\left\langle \frac{\pi F(\cos k_x, \cos k_y)}{\sqrt{\tilde{\epsilon}(z)^2+\tilde{\Delta}_{\boldsymbol{k}}(z)^2}}\right\rangle\right\rangle, \tag{18}$$

where $F(\cos k_x, \cos k_y)$ is an arbitrary function. The angular average on the Fermi surface is calculated as

$$\langle\langle\cdots\rangle\rangle = \int_0^{2\pi} \frac{d\phi}{2\pi}\frac{N_\phi}{N_0}\cdots, \tag{19}$$

where $N_\phi = k_F(\phi)/[2\pi v_F(\phi)]$ with $k_F(\phi)$ $[v_F(\phi)]$ being the angular-dependent Fermi wave-vector (velocity). Further, we approximate the temperature dependence of the gap $\Delta_x(T)$ as

$$\Delta_x(T) = \Delta_x(0)\tanh\left(\frac{\alpha}{\Delta_x(0)}\sqrt{\frac{T_c}{T}-1}\right). \tag{20}$$

Actually, $\Delta_x(0)$ slightly depends on impurity concentration, but we neglect the dependence here. We use, for $v_y=v_x$, $\Delta_x(0) \simeq 1.5T_c$, and $v_y=0.4v_x$, $\Delta_x(0) \simeq 2.2T_c$. For both cases, $\alpha/\Delta_x(0) \simeq 3.0$ is used. We then put $\Delta_y(T)=r_y\Delta_x(T)$. For $r_y$, we use the value at $T=T_c$. Actually, $r_y$ is found to depend on temperature only weakly. These approximations do not alter the conclusions given below.

Figures 4–6 show the calculated density of states $N(\omega)$ in an extended $s$-wave superconductor with impurities. At $v_y=v_x$, the order parameter is close to $d$-wave one ($A_0=0.96$), and the impurity effect on the density of states is similar to that in a $d$-wave state, in the clean case, as is shown in Fig. 4(a). At $\Gamma_B=0.076T_c^{(0)} \simeq 0.04\Delta_{\min}(0)$, only in the very close vicinity of $T_c$, $T/T_c \gtrsim 0.999\,93$, does a full gap open. In most of the region below $T_c$, the density of states is quite close to the one in the clean limit $\Gamma_B=0$, as $N(0)$ is at most around $0.001/t_x$ (at $T \simeq 0.9995T_c$) and exponentially small at lower temperatures.[31,32] In a dirtier case $[\Gamma_B=0.606T_c^{(0)} \simeq 0.6\Delta_{\min}(0)]$ (Fig. 4), remarkable features specific to an extended $s$-wave superconductors with nodes emerge. In the vicinity of $T_c$, a full gap opens in the density of states, and then a large finite density of states $N(0)$ at the chemical potential remains at low temperatures.

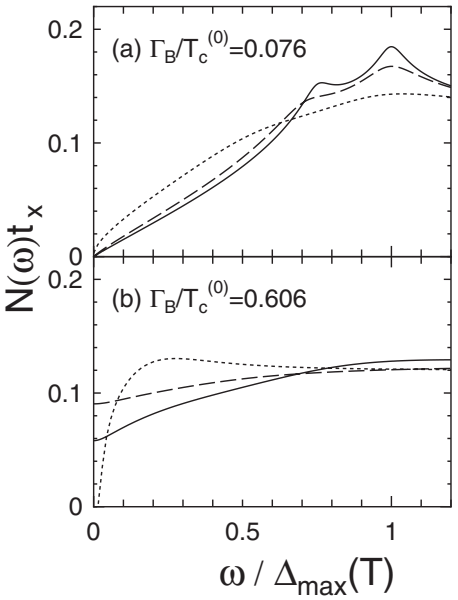


FIG. 4. Quasiparticle density of states $N(\omega)$ in an impure extended $s$-wave superconductor $[v_y=v_x(A_0=0.96)]$ for (a) $\Gamma_B/T_c^{(0)}=0.076$ $(T_c/T_c^{(0)}=0.88)$ and (b) 0.606 (0.49) at different temperatures: $T=0.99T_c$ (dotted curves), $0.9T_c$ (dashed curves), and $0.2T_c$ (solid curves). The abscissa stands for frequency $\omega$ normalized by the maximum value $\Delta_{\max}$ of the gap parameter $\Delta_{\boldsymbol{k}}$ on the Fermi surface.

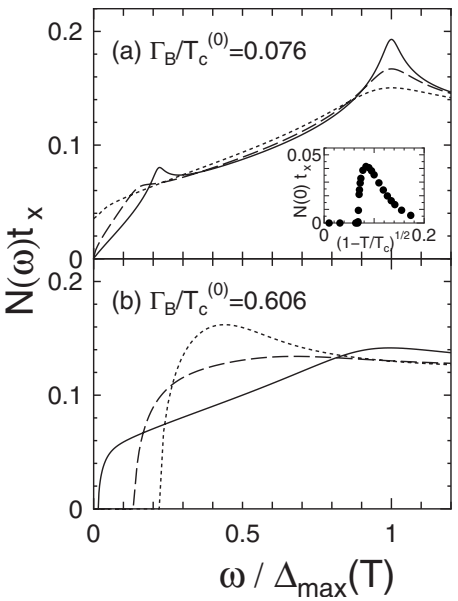


FIG. 5. Quasiparticle density of states $N(\omega)$ in an impure extended $s$-wave superconductor $[v_y=0.4v_x(A_0=0.58)]$ for (a) $\Gamma_B/T_c^{(0)}=0.076$ $(T_c/T_c^{(0)}=0.96)$ and (b) 0.606 (0.68) at different temperatures: $T=0.99T_c$ (dotted curves), $0.9T_c$ (dashed curves), and $0.2T_c$ (solid curves). The abscissa stands for frequency $\omega$ normalized by the maximum value $\Delta_{\max}$ of the gap parameter $\Delta_{\boldsymbol{k}}$ on the Fermi surface. The inset in (a) shows $N(0)$ as a function of $\sqrt{1-T/T_c}$.

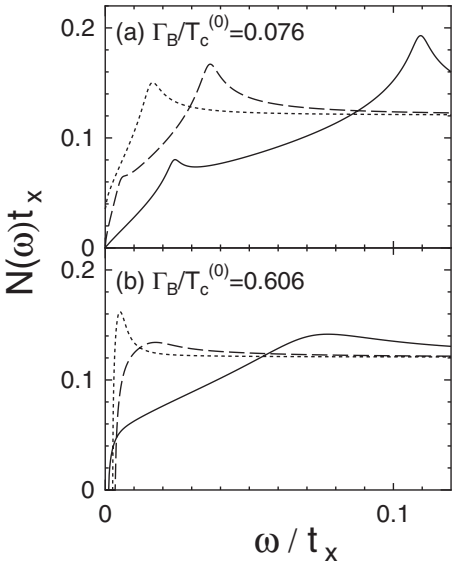


FIG. 6. Quasiparticle density of states $N(\omega)$ in an impure extended $s$-wave superconductor $[v_y=0.4v_x(A_0=0.58)]$ for (a) $\Gamma_B/T_c^{(0)}=0.076$ and (b) 0.606 at different temperatures: $T=0.99T_c$ (dotted curves), $0.9T_c$ (dashed curves), and $0.2T_c$ (solid curves). The abscissa stands for frequency $\omega$ normalized by the transfer $t_x$.

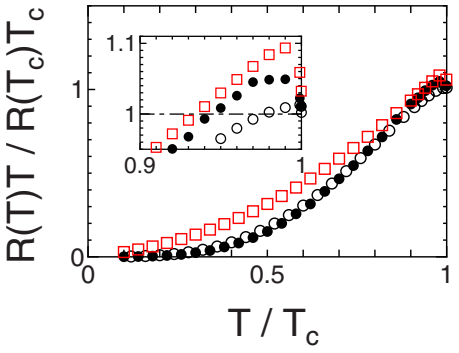


FIG. 7. (Color online) Nuclear magnetic relaxation rate $R(T)T$ $(\propto 1/T_1)$ in the superconducting state at $v_y=v_x$ $(A_0=0.96)$ for different impurity concentrations: $\Gamma_B/T_c^{(0)}=0$ (solid dots), 0.152 (open dots), and 0.606 (open squares). The inset shows the blowup near $T_c$.

At $v_y=0.4v_x$, the order parameter is less anisotropic $(A_0=0.58)$. In a fairly clean case $[\Gamma_B=0.076T_c^{(0)}\simeq 0.2\Delta_{\min}(0)$ and $T_c/T_c^{(0)}=0.96]$, a finite gap opens, as shown in the inset of Fig. 5(a), at $T>0.9955T_c$, and the density of states is gapless at lower temperatures [Fig. 5(a)]. At $T=0.9T_c$ and $0.2T_c$, $N(0)$ is finite, but it is exponentially small.[31,32] In a rather dirty case $[\Gamma_B=0.606T_c^{(0)}\simeq 2\Delta_{\min}(0)$ and $T_c/T_c^{(0)}=0.68]$, a finite gap always develops [Fig. 5(b)]. In particular, at $T=0.99T_c$, a sharp peak in the density of states on the edge of the finite gap is beginning to develop [Fig. 6(b)].

### C. Nuclear magnetic relaxation time $1/T_1$

The peculiar behavior of the density of states at low energies must cause interesting behavior of other quantities. In particular, the nuclear magnetic relaxation time $1/T_1$ must exhibit peculiar temperature dependence as a function of impurity concentration. The relaxation time $1/T_1$ is given by[35]

$$\frac{1}{T_1} \propto \frac{T}{N}\sum_{\boldsymbol{q}} |A(\boldsymbol{q})|^2 \lim_{\omega\to 0}\frac{1}{\omega}\mathrm{Im}\,\chi(\boldsymbol{q},\omega+i\delta), \tag{21}$$

where $\chi(\boldsymbol{q},\omega+i\delta)$ is dynamical (transverse) spin susceptibility, and $A(\boldsymbol{q})$ is the hyperfine coupling between a nuclear spin and a conduction electron. Impurity potential causes not only self-energy correction, but also vertex correction for the spin susceptibility, but the latter can be safely neglected in calculating $1/T_1$,[36,37] (although there is also a report that the impurity vertex correction causes enhancement of the coherence peak[38]). Then, the relaxation rate $R(T)[\propto 1/(T_1T)]$ is given by

$$R(T) = \frac{1}{N}\sum_{\boldsymbol{q}} \lim_{\omega\to 0}\frac{1}{\omega}\mathrm{Im}\,\chi(\boldsymbol{q},\omega+i\delta)$$
$$= \frac{4}{\pi}\int_0^\infty d\epsilon\left(-\frac{df}{d\epsilon}\right)[g_0''(\epsilon+i\delta)^2+g_x''(\epsilon+i\delta)^2], \tag{22}$$

where $f$ is the Fermi distribution function. In Fig. 7, we show $R(T)T$ $(\propto 1/T_1)$ for $v_y=v_x$ and different impurity concentrations. In this case, the gap parameter is quite close to the $d$-wave one. In the clean limit, there occurs a weak coherence peak just below $T_c$. Adding a small amount of impurities almost diminishes the coherence peak (see the inset). This is similar to the behavior in a $d$-wave superconductor.[6] There occurs no coherence peak in a clean $d$-wave superconductor, and impurities further suppress $1/T_1$ below $T_c$. Strictly speaking, a finite gap in the density of states is present just below $T_c$ (as was shown in Sec. III B), but its effect is limited and invisible in the present case. On further increasing impurity concentration, a clear coherence peak develops below $T_c$, in contrast to a $d$-wave case. Impurity-induced development of a coherence peak is a common phenomenon in anisotropic $s$-wave superconductor.[39] However, the coherence peak does not yet fully develop in the present case.

At low temperatures, $1/T_1$ varies in proportion to $T^3$ in the clean cases as a result of nodes of the gap (see also Fig. 10). At finite impurity concentration, $N(0)$ is finite, but its effect is negligible because it is exponentially small. On the other hand, in the dirty case $(\Gamma_B/T_c=0.606, T_c/T_c^{(0)}\simeq 0.5)$, $1/T_1$ is roughly proportional to $T$, reflecting a finite $N(0)$. In this case, $\Gamma_B$ is large, but not yet large enough for inequality $\Gamma_B>\Delta_{\min}(0)$ to hold. That is why a finite $N(0)$ is obtained. For a larger $\Gamma_B$, a full gap is realized at any temperatures below $T_c$, and exponential dependence of $1/T_1$ on $T$ would be observed. However, $T_c$ itself has already been very much reduced then.

At $v_y=0.4v_x$, the gap parameter is more isotropic $(A_0=0.58)$. In this case, introduction of impurities readily enhances the coherence peak below $T_c$ as shown in Fig. 8. In the clean case, $1/T_1$ varies proportionally to $T^3$ at low tem-

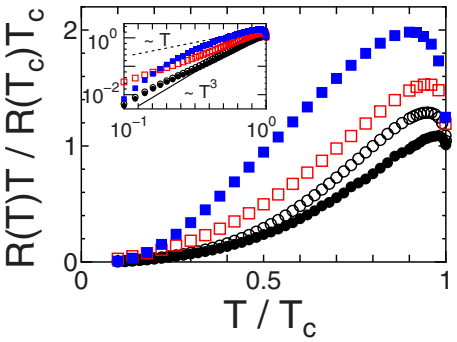


FIG. 8. (Color online) Nuclear magnetic relaxation rate $R(T)T$ ($\propto 1/T_1$) in the superconducting state at $v_y=0.4v_x$ ($A_0=0.58$) for different impurity concentrations: $\Gamma_B/T_c^{(0)}=0$ (solid dots), 0.076 (open dots), 0.606 (open squares), and 1.213 (solid squares). The inset shows log-log plot.

peratures. In the dirty case ($\Gamma_B/T_c^{(0)}=1.213$), $1/T_1$ decreases more rapidly because the full gap is opened by impurities at low temperatures (see the inset). At $\Gamma_B/T_c^{(0)}=0.606$, as temperature decreases, $1/T_1$ decreases rather slowly. It is quite close to the $T$-linear variation. In this case, a full gap opens, but its magnitude is so small (see Fig. 5) that the exponential behavior is not yet clearly seen. At lower temperatures, it must decrease exponentially.

The results for $1/T_1$ is summarized schematically in Fig. 9.

## IV. SUMMARY

We have shown that, in a crystal of low symmetry, an extended $s$-wave superconducting state with order parameter changing its sign on the Fermi surface is likely to occur if the pairing interaction is of the electronic origin. Since, in some of organic conductors, these conditions are likely to be satisfied, it is expected that an extended $s$-wave pairing is realized in those organic superconductors.

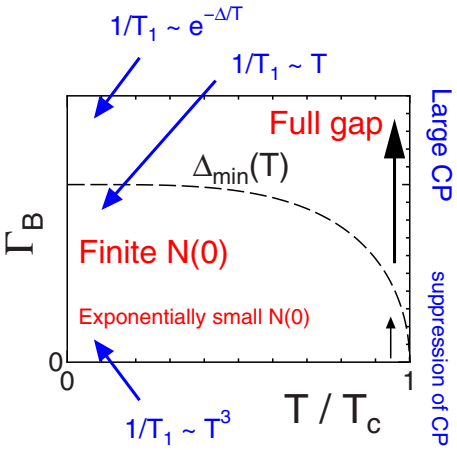


FIG. 9. (Color online) Qualitative behavior of the nuclear relaxation rate $1/T_1$ in a 2D extended $s$-wave superconductor with sign-changing order parameter $\Delta_k$, $-\Delta_{\min}(T)\leq\Delta_{k_F}\leq\Delta_{\max}(T)$ [$\Delta_{\min}(T)\geq 0$] in the presence of weak scattering potential. The abscissa is $T/T_c$, and the ordinate is the scattering rate $\Gamma_B$. Dashed curve stands for $\Delta_{\min}(T)$. CP stands for coherence peak.

The change in the sign of the order parameter means that the gap parameter $\Delta_k$ takes values in the region of $-\Delta_{\min}(T)\leq\Delta_{k_F}\leq\Delta_{\max}(T)$ with $\Delta_{\min}(T)$, $\Delta_{\max}(T)>0$ on the Fermi surface. The transition temperature $T_c$ and the temperature dependence of $\Delta_{\min}(T)$ are determined, once the scattering rate $\Gamma_B$ is given, and we can show the temperature dependence of $\Delta_{\min}(T)$ as a function of $T/T_c$ as in Fig. 9. As the gap parameter approaches to an isotropic one, $\Delta_{\min}(T)$ decreases. Negative $\Delta_{\min}(T)$ implies a fully gapped order parameter. If $\Gamma_B\gtrsim\Delta_{\min}(T)$ [see Eq. (17) for the precise condition], a full gap opens in the density of states, $N(0)=0$. Otherwise, the density of states is gapless, $N(0)>0$, although $N(0)$ is exponentially small at $\Gamma_B\ll\Delta_{\min}(T)$, in the weak scattering case.[31,32]

Behavior of $1/T_1$ in an extended $s$-wave superconductor with sign-changing order parameter (on the Fermi surface) in the presence of weak scatterers is summarized as follows (see Fig. 9): (1) in the absence of impurities, $1/T_1$ has a weak coherence peak, and follows $T^3$-power law at low temperatures. (2) In the clean case, $\Gamma_B\ll\Delta_{\min}(0)$, the coherence peak below $T_c$ is weakly suppressed. (However, it is enhanced as $\Gamma_B$ further increases.) $1/T_1$ varies roughly proportionally to $T^3$ at low temperatures. (3) At $\Gamma_B\lesssim\Delta_{\min}(0)$, a coherence peak develops below $T_c$, and $1/T_1$ is proportional to $T$ at low temperatures. (4) At $\Gamma_B\gg\Delta_{\min}(0)$, a prominent coherence peak is observed, and $1/T$ decreases exponentially at low temperatures.

Width of observability window depends on the anisotropy $A_0$ of the gap. If $1-A_0\ll 1$, i.e., if it is very anisotropic, the system stays mostly in the regions (1)–(3). Ultimately, region (4) is reached. However, then, $T_c$ has already been very much reduced from $T_c^{(0)}$, and the observability of region (4) is rather limited. On the other hand, if $A_0\ll 1$, region (4) is readily reached, and observability of regions (2) and (3) is limited.

Region (2) is specific to the case with weak scattering potential. If scattering potential is strong enough, $1/T_1$ becomes proportional to $T$ in the presence of small amount of impurities (See Appendix A).

In triclinic systems such as many of $\alpha$- or $\beta$-(BEDT-TTF) salts (where BEDT-TTF stands for bis(ethylenedithio)tetrathiafulvalence) and $(TMTSF)_2X$ (where TMTSF stands for tetramethyltetraselenafulvalene), there is only one irreducible representation corresponding to the singlet pairing. Therefore, if the gap has nodes, the order parameter must be an extended $s$-wave one with sign change, and the present theory must be always applicable. It is highly desirable that the transition temperature and $1/T_1$ as a function of impurities will be systematically measured in those systems.

In cases with crystals of higher symmetry, the present theory can also be helpful in identifying the symmetry of order parameter. For example, $\kappa$-$(BEDT\text{-}TTF)_2Cu(NCS)_2$ is an organic superconductor of monoclinic symmetry. The point group describing its symmetry is $C_{2h}$. It has two irreducible representations of even parity: $A_{1g}$ and $B_{1g}$. In fact, there has been controversy over the symmetry of order parameter in this material.[19] The two possibilities of order parameter symmetry are often referred to as $d_{x^2-y^2}$ and $d_{xy}$. The

$d_{x^2-y^2}$ state belongs to the $B_{1g}$ representation, and $d_{xy}$ to the $A_{1g}$, i.e., $d_{xy}$ state is actually an extended $s$-wave state.[40] The experimental results of the dependence of the transition temperature on the interlayer residual resistivity are qualitatively similar to Fig. 3,[41] implying the order parameter is an extended $s$-wave one (with small $A_0$). Nuclear magnetic relaxation time was also measured in this material.[42] No coherence peak was observed below $T_c$, but anomalous large peak at far below $T_c$, probably caused by vortex motion,[43] made it difficult to observe the temperature dependence of $1/T_1$ (without contributions from vortex motion). A systematic study of $1/T_1$ would be helpful in identifying the order parameter symmetry if the contribution from vortex motion is suppressed.

## APPENDIX A: SELF-CONSISTENT $T$-MATRIX APPROXIMATION

In the self-consistent $t$-matrix approximation, Eq. (9) is replaced by

$$i\tilde{\epsilon}(i\epsilon_n) = i\epsilon_n + \frac{n_i g_0(i\epsilon_n)}{u^{-2} - g_0(i\epsilon_n)^2 + g_x(i\epsilon_n)^2}, \tag{A1}$$

and Eq. (10) by

$$\tilde{\Delta}_k(i\epsilon_n) = \Delta_k + \frac{n_i g_x(i\epsilon_n)}{u^{-2} - g_0(i\epsilon_n)^2 + g_x(i\epsilon_n)^2}. \tag{A2}$$

In the unitarity limit, $u \to \infty$,

$$i\tilde{\epsilon}(i\epsilon_n) = i\epsilon_n - \frac{n_i g_0(i\epsilon_n)}{g_0(i\epsilon_n)^2 - g_x(i\epsilon_n)^2}, \tag{A3}$$

and

$$\tilde{\Delta}_k(i\epsilon_n) = \Delta_k - \frac{n_i g_x(i\epsilon_n)}{g_0(i\epsilon_n)^2 - g_x(i\epsilon_n)^2}. \tag{A4}$$

In the unitarity limit, the same result as that in the Born limit is obtained for the dependence of the transition temperature on the impurity concentration except for the replacement of $\Gamma_B$ with $\Gamma = n_i/[\pi N_0]$. However, the density of states at low energy is quite different from those in the Born limit, because strong potential scattering causes a resonance at a low energy (at the chemical potential in the particle-hole symmetric case) and it gives rise to a finite density of states at the chemical potential proportional to $\sqrt{n_i}$.[33,34] This has a significant effect on the nuclear relaxation rate $1/T_1$. Even in the case with $\Gamma \ll \Delta_{\min}(0)$, $1/T_1 \simeq T$ because of non-negligible density of states at $\omega = 0$ (see Fig. 10).

## APPENDIX B: DEPENDENCE OF TRANSITION TEMPERATURE ON THE IMPURITY CONCENTRATION

In analytic calculations, we use the approximation [Eq. (18)]. Then, defining $C_\mu$ and $C_{\mu\nu}$ as $C_\mu = \langle\langle \cos k_\mu \rangle\rangle$ and $C_{\mu\nu} = \langle\langle \cos k_\mu \cos k_\nu \rangle\rangle$, we find that the equation determining $T_c$ is given by

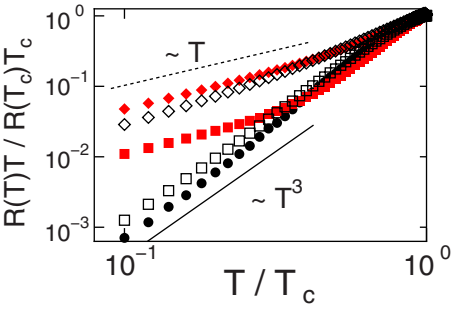


FIG. 10. (Color online) Nuclear magnetic relaxation rate $R(T)T$ ($\propto 1/T_1$) in the superconducting state at $v_y = v_x$ ($A_0 = 0.96$) for different impurity concentrations: $\Gamma/T_c^{(0)} = 0$ (solid dots), 0.152 (solid squares), and 0.606 (solid diamonds), where $\Gamma = n_i/[\pi N_0]$. For comparison, the results in the Born approximation are shown by open symbols: $\Gamma_B/T_c^{(0)} = 0.152$ (open squares) and 0.606 (open diamonds).

$$\begin{vmatrix} 1 - \tilde{v}_x(C_{xx}\delta\Psi + Gc_x^2) & -\tilde{v}_x(C_{xy}\delta\Psi + Gc_xc_y) \\ -\tilde{v}_y(C_{xy}\delta\Psi + Gc_xc_y) & 1 - \tilde{v}_y(C_{yy}\delta\Psi + Gc_y^2) \end{vmatrix} = 0, \tag{B1}$$

where $\tilde{v}_\mu = N_0 v_\mu$, $\delta\Psi = \Psi(N_c + \frac{1}{2} + \frac{\Gamma_B}{2\pi T_c}) - \Psi(\frac{1}{2} + \frac{\Gamma_B}{2\pi T_c})$, $G = \Psi(\frac{1}{2} + \frac{\Gamma_B}{2\pi T_c}) - \Psi(\frac{1}{2})$, $\Psi(z)$ is the digamma function, and $N_c = W/(2\pi T_c)$ with $W$ being a high-frequency cut-off of the order of the band width.

First, we calculate the gap anisotropy $A_0$ in the limit of $T \to T_c^{(0)}$, i.e., in the clean limit. We can easily show that

$$\frac{\Delta_y}{\Delta_x} = \frac{v/v_x - C_{xx}}{C_{xy}} = \frac{C_{xy}}{v/v_y - C_{yy}}, \tag{B2}$$

where $1/(N_0 v) = \delta\Psi^{(0)} = \Psi(N_c^{(0)} + \frac{1}{2}) - \Psi(\frac{1}{2})$ with $N_c^{(0)} = W/(2\pi T_c^{(0)})$. Using Eq. (B2), we can show that

$$A_0 = \frac{(v/v_y - C_{yy})\delta_{xx} + (v/v_x - C_{xx})\delta_{yy} + 2C_{xy}\delta_{xy}}{v(C_{xx}/v_y + C_{yy}/v_x) - (C_{xx}C_{yy} - C_{xy}^2)}, \tag{B3}$$

where $\delta_{\mu\nu} = C_{\mu\nu} - C_\mu C_\nu$.

Now, we calculate the transition temperature $T_c$. We note that the cutoff energy $W$ is much (exponentially) larger than $T_c^{(0)}$ and $T_c$, and that $\Gamma_B \simeq T_c^{(0)}$ (We cannot apply the present theory to the case with $\Gamma_B \sim W$). Therefore, we can use the inequality $\delta\Psi - \delta\Psi^{(0)}$, $G \ll \delta\Psi^{(0)}$, $\delta\Psi$. We can thus put $\delta\Psi + \delta\Psi^{(0)} \simeq 2\delta\Psi^{(0)} = 2/(N_0 v)$, for example. Using Eqs. (B1) and (B2), then, we obtain

$$\delta\Psi - \delta\Psi^{(0)} = \ln\frac{T_c^{(0)}}{T_c} = A_0 G = A_0\left[\Psi\left(\frac{1}{2} + \frac{\Gamma_B}{2\pi T_c}\right) - \Psi\left(\frac{1}{2}\right)\right]. \tag{B4}$$

Equations (14) and (15) are derived from Eq. (B4).

[1] P. W. Anderson, J. Phys. Chem. Solids **11**, 26 (1959).
[2] A. A. Abrikosov and L. P. Gor'kov, Zh. Eksp. Teor. Fiz. **39**, 1781 (1960); Sov. Phys. JETP **12**, 1243 (1961).
[3] G. E. Volovik and L. P. Gor'kov, Zh. Eksp. Teor. Fiz. **88**, 1412 (1985); Sov. Phys. JETP **61**, 843 (1985).
[4] J. F. Annett, Adv. Phys. **39**, 83 (1990).
[5] M. Sigrist and K. Ueda, Rev. Mod. Phys. **63**, 239 (1991).
[6] T. Hotta, J. Phys. Soc. Jpn. **62**, 274 (1993).
[7] L. S. Borkowski and P. J. Hirschfeld, Phys. Rev. B **49**, 15404 (1994).
[8] R. Fehrenbacher and M. R. Norman, Phys. Rev. B **50**, 3495 (1994).
[9] D. S. Hirashima, Phys. Rev. B **50**, 10142 (1994).
[10] R. Fehrenbacher and M. R. Norman, Physica C **235-240**, 2407 (1994).
[11] A. A. Abrikosov, Physica C **244**, 243 (1995).
[12] S. V. Pokrovsky and V. L. Pokrovsky, Phys. Rev. Lett. **75**, 1150 (1995).
[13] S. V. Pokrovsky and V. L. Pokrovsky, Phys. Rev. B **54**, 13275 (1996).
[14] G. Preosti and P. Muzikar, Phys. Rev. B **54**, 3489 (1996).
[15] For example, D. A. Wollman, D. J. Van Harlingen, W. C. Lee, D. M. Ginsberg, and A. J. Leggett, Phys. Rev. Lett. **71**, 2134 (1993); C. C. Tsuei, J. R. Kirtley, C. C. Chi, Lock See Yu-Jahnes, A. Gupta, T. Shaw, J. Z. Sun, and M. B. Ketchen, *ibid.* **73**, 593 (1994); A. Mathai, Y. Gim, R. C. Black, A. Amar, and F. C. Wellstood, *ibid.* **74**, 4523 (1995).
[16] T. Ishiguro, K. Yamaji, and G. Saito, *Organic Superconductors* (Springer, Berlin, 1997).
[17] J. Wosnitza, *Fermi Surfaces of Low-Dimensional Organic Metals and Superconductors* (Springer, Berlin, 1996).
[18] Y. Yanase, T. Jujo, T. Nomura, H. Ikeda, T. Hotta, and K. Yamada, Phys. Rep. **387**, 1 (2003).
[19] K. Kuroki, J. Phys. Soc. Jpn. **75**, 051013 (2006).
[20] J. Schmalian, Phys. Rev. Lett. **81**, 4232 (1998).
[21] H. Kino and H. Kontani, J. Phys. Soc. Jpn. **67**, 3691 (1998).
[22] H. Kondo and T. Moriya, J. Phys. Soc. Jpn. **67**, 3695 (1998).
[23] J. Merino and R. H. McKenzie, Phys. Rev. Lett. **87**, 237002 (2001).
[24] A. Kobayashi, Y. Tanaka, M. Ogata, and Y. Suzumura, J. Phys. Soc. Jpn. **73**, 1115 (2004).
[25] S. Onari, R. Arita, K. Kuroki, and H. Aoki, Phys. Rev. B **70**, 094523 (2004).
[26] Y. Tanaka, Y. Yanase, and A. Kobayashi, J. Phys. Soc. Jpn. **73**, 2053 (2004).
[27] A. Kobayashi, Y. Suzumura, M. Higa, R. Kondo, S. Kagoshima, and H. Nishikawa, J. Phys.: Condens. Matter **20**, 12505 (2008).
[28] T. Tsuneto, Prog. Theor. Phys. **28**, 857 (1962).
[29] D. Markowitz and L. P. Kadanoff, Phys. Rev. **131**, 563 (1963).
[30] P. Hohenberg, Zh. Eksp. Teor. Fiz. **45**, 1208 (1963); Sov. Phys. JETP **18**, 834 (1964).
[31] L. P. Gor'kov and P. A. Kalugin, Pis'ma Zh. Eksp. Teor. Fiz. **41**, 208 (1985); JETP Lett. **41**, 253 (1985).
[32] K. Ueda and T. M. Rice, in *Theory of Heavy Fermions and Valence Fluctuations*, edited by T. Kasuya and T. Saso (Springer, Berlin, 1985), p.267.
[33] S. Schmitt-Rink, K. Miyake, and C. M. Varma, Phys. Rev. Lett. **57**, 2575 (1986).
[34] P. J. Hirschfeld, D. Vollhardt, and P. Wölfle, Solid State Commun. **59**, 111 (1986).
[35] T. Moriya, Prog. Theor. Phys. **28**, 371 (1962).
[36] K. Maki and P. Fulde, Phys. Rev. **140**, A1586 (1965).
[37] K. V. Samokhin and B. Mitrović, J. Phys.: Condens. Matter **19**, 026210 (2007).
[38] H.-Y. Choi and E. J. Mele, Phys. Rev. B **52**, 7549 (1995).
[39] Y. Masuda, Phys. Rev. **126**, 1271 (1962).
[40] B. J. Powell, J. Phys.: Condens. Matter **18**, L575 (2006).
[41] J. G. Analytis, A. Ardavan, S. J. Blundell, R. L. Owen, E. F. Garman, C. Jeynes, and B. J. Powell, Phys. Rev. Lett. **96**, 177002 (2006).
[42] T. Takahashi, T. Tokiwa, K. Kanoda, H. Urayama, H. Yamochi, and G. Saito, Physica C **153-155**, 487 (1988).
[43] T. Takahashi, K. Kanoda, K. Akiba, K. Sakao, M. Watabe, K. Suzuki, and G. Saito, Synth. Met. **42**, 2005 (1991).